RESEARCH ARTICLE

Age-disproportionate atrophy in Alzheimer's disease and Parkinson's disease spectra

Kenji Yoshinaga[1,2] | Toma Matsushima[2,3] | Mitsunari Abe[2] | Tsunehiko Takamura[2,4] | Hiroki Togo[1,2] | Noritaka Wakasugi[2] | Nobukatsu Sawamoto[5,6] | Toshiya Murai[7] | Toshiki Mizuno[8] | Teruyuki Matsuoka[9,10] | Kazuaki Kanai[11] | Hiroshi Hoshino[12] | Atsushi Sekiguchi[2,4] | Nobuo Fuse[13] | Shunji Mugikura[13] | Tohoku Medical Megabank Brain Magnetic Resonance Imaging Study (TMMbMRI)Parkinson's and Alzheimer's disease Dimensional Neuroimaging Initiative (PADNI) | Takashi Hanakawa[1,2]

[1]Department of Integrated Neuroanatomy and Neuroimaging, Kyoto University Graduate School of Medicine, Kyoto, Japan

[2]Department of Advanced Neuroimaging, Integrative Brain Imaging Center, National Center of Neurology and Psychiatry, Kodaira, Tokyo, Japan

[3]Department of Biotechnology and Life Science, Tokyo University of Agriculture and Technology, Bunkyo-ku, Tokyo, Japan

[4]Department of Behavioral Medicine, National Institute of Mental Health, National Center of Neurology and Psychiatry, Kodaira, Tokyo, Japan

[5]Department of Human Health Sciences, Kyoto University Graduate School of Medicine, Kyoto, Japan

[6]Department of Neurology, Kyoto University Graduate School of Medicine, Kyoto, Japan

[7]Department of Psychiatry, Kyoto University Graduate School of Medicine, Kyoto, Japan

[8]Department of Neurology, Graduate School of Medical Science, Kyoto Prefectural University of Medicine, Kyoto, Japan

[9]Department of Psychiatry, Graduate School of Medical Science, Kyoto Prefectural University of Medicine, Kyoto, Japan

[10]Department of Psychiatry, NHO Maizuru Medical Center, Maizuru, Kyoto, Japan

[11]Department of Neurology, Fukushima Medical University, Fukushima, Japan

[12]Department of Neuropsychiatry, Fukushima Medical University, Fukushima, Japan

[13]Tohoku Medical Megabank Organization, Tohoku University, Sendai, Japan

Correspondence
Takashi Hanakawa, Department of Integrated Neuroanatomy and Neuroimaging, Kyoto University Graduate School of Medicine, Yoshida-Konoe, Sakyo-ku, Kyoto, 606-8501, Japan.
Email: hanakawa.takashi.2s@kyoto-u.ac.jp

Abstract

INTRODUCTION: Brain age gap (BAG), defined as the difference between MRI-predicted 'brain age' and chronological age, can capture information underlying various neurological disorders. We investigated the pathophysiological significance of the BAG across neurodegenerative disorders.

METHODS: We developed a brain age estimator using structural MRIs of healthy-aged individuals from one cohort study. Subsequently, we applied this estimator to people with Alzheimer's disease spectra (AD) and Parkinson's disease (PD) from another cohort study. We investigated brain sources responsible for BAGs among these groups.

Kenji Yoshinaga, Toma Matsushima, and Takashi Hanakawa contributed equally to this study.

RESULTS: Both AD and PD exhibited a positive BAG. Brain sources showed overlapping, yet partially segregated, neuromorphological differences between these groups. Furthermore, employing with t-distributed stochastic neighbor embedding on the brain sources, we subclassified PD into two groups with and without cognitive impairment.

DISCUSSION: Our findings suggest that brain age estimation becomes a clinically relevant method for finely stratifying neurodegenerative disorders.

KEYWORDS
cognitive impairment, cohort, imaging markers, machine learning, MRI

Highlights

- Brain age estimated from structure MRI data was greater than chronological age in patients with Alzheimer's disease/mild cognitive impairment or Parkinson's disease.
- Brain regions attributed to brain age estimation were located mainly in the fronto-temporo-parietal cortices but not in the motor cortex or subcortical regions.
- Brain sources responsible for the brain age gaps revealed roughly overlapping, yet partially segregated, neuromorphological differences between participants with Alzheimer's disease/mild cognitive impairment and Parkinson's disease.
- Participants with Parkinson's disease were subclassified into two groups (with and without cognitive impairment) based on brain sources responsible for the brain age gaps.

1 | BACKGROUND

Brain MRIs of individuals with Alzheimer's disease (AD) often appear older than patients' chronological age. Such a pathological change in brain morphology occurs in addition to the normative neuromorphological changes that arise dynamically throughout the human lifespan.[1] Technological advances have enabled the assessment of dynamic age-related neuromorphological changes using MRI scans, which can be non-invasively acquired from fetuses to centenarians to form large-scale databases.[1–3] The application of machine learning algorithms to magnetic resonance imaging (MRI) features (e.g., cortical thickness, gray matter volume) has enabled the development of a brain age estimation (BAE) method, which is designed to estimate an individual's chronological age from their brain MRI images.[4,5] The difference between brain age and chronological age is called the brain age gap (BAG).

A positive BAG, which typically indexes excessive brain aging, has been reported in people with cognitive decline[6] and AD.[7–12] Moreover, positive BAGs have also been reported in people with Parkinson's disease (PD)[11,13,14] and neuropsychiatric disorders.[15,16] Nevertheless, if disease-specific information can be extracted from BAG-related neuromorphological features, BAE technology may further our understanding of neurodegenerative disorders. Specifically, by back-projecting the correlates of the BAG to the original feature space

in the brain, it may be possible to differentially attribute BAGs to various disorders, such as AD and PD. Such spatial characterization could then be followed by the stratification or deep profiling of as yet unidentified disease subgroups. This approach would be particularly powerful when combined with the BAE procedure because BAE removes the effects of normative aging, which is a confounder of disease effects.

To gain deeper insight into the pathophysiology of AD and PD, we investigated neuromorphological changes responsible for the BAG in these diseases using two large MRI datasets. We built our BAE predictor using the dataset from the Tohoku Medical Megabank Brain MRI (TMMbMRI) study,[17] which is the largest community-based MRI cohort in Japan. We applied the BAE predictor to the MRIs of people with AD, PD, and healthy aging in the independent cohort, the Parkinson's and Alzheimer's disease Dimensional Neuroimaging Initiative (PADNI).[18–20] We computed the BAG among these groups and analyzed its relationship with clinical batteries. We further compared the brain sources of the BAG across these groups. Through these analyses, we tested the following hypotheses. First, the BAE method would yield positive BAGs when applied to either AD or PD patients. Second, the brain sources responsible for the BAG would reflect distinct neuromorphological differences among healthy aging individuals and patients with AD and PD. Finally, the BAG and its sources convey some information about clinical symptoms such as cognitive impairment.

2 | METHODS

2.1 | Participants and MRI data acquisition

We recruited healthy individuals aged over 40 years from the TMMbMRI study.[17] Based on the inclusion and exclusion criteria,[21] we selected MRI data from 2707 adults aged over 40 years to build the BAE model (see Table 1 and Figure S1 for the demographic data). All participants were independent individuals who voluntarily agreed to participate and were able to visit the study sites independently. For individuals aged ≥ 65 years, those with a Mini-Mental State Examination (MMSE) score < 27 were excluded. The details of this content are provided in Section 1 of Supporting Information.

The PADNI cohort comprises data acquired from participants aged ≥ 50 years old across four sites in Japan: the National Centre of Neurology and Psychiatry (NCNP), Kyoto University (KU), Kyoto Prefectural University of Medicine (KPUM), and Fukushima Medical University (FMU). We analyzed interim PADNI data acquired from 85 healthy older adults (PADNI HA hereafter), 94 patients with PD, 13 patients with AD, and 35 patients with mild cognitive impairment (MCI) (see Table 1 and Figure S1 for the demographic data). The diagnoses of AD/MCI and PD were conducted according to the National Institute on Aging-Alzheimer's Association AD diagnostic guidelines[22] and the International Parkinson and Movement Disorder Society (MDS) criteria,[23] respectively. Due to the small numbers of participants, the MCI and AD groups were combined because of the small numbers of participants (AD/MCI hereafter). The details of this content are provided in Section 1 of Supporting Information and Table S1.

T1-weighted 3D structural MRI data were obtained using a magnetization prepared-rapid gradient echo sequence in both the TMMbMRI study and the PADNI cohort (according to the Brain/MINDS harmonization protocol[24]). The detailed sequence parameters are listed in Table 1.

All PADNI participants underwent a neuropsychological/clinical battery, which comprised the clinical dementia rating (CDR), MMSE, Montreal Cognitive Assessment-Japanese version (MoCA), immediate recall (IR) and delayed recall (DR) of the logical memory (LM) and visual reproduction (VR) subtests of the Wechsler Memory Scale-Revised (WMS-R) and MDS sponsored revision of Unified Parkinson's Disease Rating Scale (MDS-UPDRS).

2.2 | MRI data preprocessing

We used the *recon-all* command of FreeSurfer v6.0 to segment the structural MRI data. The cerebral cortex was subdivided into 148 regions according to the Destrieux Atlas.[25] The Aseg Atlas[26] was used to subdivide the subcortical structures into 45 regions, from which only subcortical gray matter volumes (ScV) were selected (i.e., 19 regions listed in Table S2) and subjected to further analyses. All 167 MRI features (cortical thickness for the 148 cortical regions and ScV for the 19 subcortical gray matter regions) were fed into our BAE model after correcting for scanner/site differences using combatting batch effects when combining batches of gene expression microarray data

RESEARCH IN CONTEXT

1. **Systematic review**: Magnetic resonance imaging (MRI)-predicted age, known as brain age, is currently under extensive investigation within the fields of neurology and neuroscience. Previous studies have successfully estimated brain age using machine learning techniques and have reported an increase in the brain age gap across various neurological disorders. However, to the best of the authors' knowledge, the specific brain sources responsible for this gap have not yet been investigated. These earlier studies are appropriately cited.

2. **Interpretation**: Our findings shed light on a pathophysiological aspect of the brain age gap in neurodegenerative diseases. The brain age gap may not only serve as a supportive marker for a diagnosis but also hold potential as a marker for clinical symptoms, particularly cognitive impairment.

3. **Future directions**: The manuscript introduces new perspectives to brain age research. Investigating the brain sources responsible for the brain age gap is beneficial in the following aspects: (1) Research on the disease-specific distribution of brain sources aids in diagnosing and categorizing neurological disorders. (2) Exploring the relationship between the brain age gap and clinical symptoms. (3) Investigating potential causes for the acceleration of brain aging.

(ComBat).[27] We built a ComBat model (with age, sex, and group labels as covariates to be preserved) to remove differences in imaging properties between the twin scanners used by the TMMbMRI study and the various scanners used by the four PADNI sites.

2.3 | Brain age estimation procedure

We used a partial least squares regression (PLS) model to build the BAE model using MRI features that typically have multiple collinearities. In practice, we used Python version 3.8.2 (https://www.python.org/) and scikit-learn version 1.1.1 (https://scikit-learn.org/stable/). A 10-fold nested cross-validation (CV) scheme was used (Figure 1). Hyperparameters were tuned in the inner loop, and estimation was performed in the outer loop. The details of this content are provided in Section 2 of Supporting Information.

The accuracy of the prediction was assessed by the mean absolute error between predicted age and chronological age (MAE), coefficient of determination (R^2), and Spearman's correlation coefficient (*rho*). An estimation bias inherent to the BAE procedure was corrected using the previously established method.[28,29]

We assessed the brain features that contributed to the BAE model in the TMMbMRI dataset. From the BAE model using the entire

TABLE 1 Profiles of study participants

Parameter	TMMbMRI	PADNI		
	HA	HA	PD	AD/MCI
No. of participants	2707 (>40 yrs for Training) 2079 (≥50 yrs for Test)	85 (NCNP $n = 52$, KU $n = 23$, KPUM $n = 10$, FMU $n = 0$) (CDR 0 $n = 85$)	94 (NCNP $n = 35$, KU $n = 44$, KPUM $n = 2$, FMU $n = 13$) (CDR 0 $n = 61$; 0.5 $n = 27$; 1 $n = 5$; 2 $n = 1$)	48 (NCNP $n = 19$, KU $n = 8$, KPUM $n = 16$, FMU $n = 5$) (CDR 0.5 $n = 35$; 1 $n = 10$; 2 $n = 3$)
Sex (male/female)	980/1727 vs. PADNI HA: $\chi^2 = 11.67$, $P = 6.3*10^{-4}$	47/38 $\chi^2 = 5.20$, $P = 0.07$	49/45	17/31
Age (mean ± SD yrs, min–max)	58.2 ± 10.0, 40–80 (for Training) 62.6 ± 6.8, 50–80 (for Test)	66.7 ± 8.1, 50–80	67.7 ± 7.2, 50–80	72.0 ± 6.3, 55–80
	Test vs. PADNI HA: $t = -5.446$, $P = 5.73*10^{-8}$	$F_{[2,224]} = 8.3$, $P = 0.0003$ (HA vs. PD: $t = -0.86$, $P = 0.39$; HA vs. AD/MCI: $t = -3.91$, $P = 1.50*10^{-4}$; PD vs. AD/MCI: $t = -3.52$, $P = 5.84*10^{-4}$)		
MRI Sequence parameters	32-channel head coil on twin 3-T MRI scanners (Ingenia, Philips Medical System, Netherlands) repetition time = 11 ms, echo time = 5.2 ms, inversion time = 1068.3 ms, flip angle = 8°, matrix size = 368 × 368, and voxel size = 0.7 × 0.7 × 0.7 mm	3-T Verio Dot/Skyra Fit scanner (Siemens, Erlangen, Germany) at NCNP Skyra scanners (Siemens, Erlangen, Germany) at KU, KPUM, and FMU repetition time = 2500 ms, echo time = 2.18 ms, inversion time = 1000 ms, flip angle = 8°, matrix size = 320 × 300, and voxel size = 0.8 × 0.8 × 0.8 mm		
MMSE	28.8 ± 1.0	29.3 ± 1.1	27.9 ± 2.7	23.9 ± 5.2
	Test vs. PADNI HA: $t = -3.97$, $P = 7.6*10^{-5}$	$F_{[2,223]} = 50.04$, $P = 1.1 \times 10^{-18}$ (HA vs. PD: $t = 4.33$, $P = 2.4*10^{-5}$, HA vs. AD/MCI: $t = 9.29$, $P = 4.5*10^{-16}$, PD vs. AD/MCI: $t = 6.11$, $P = 9.4*10^{-9}$)		

Note: Mild cognitive impairment (MCI, $n = 35$) and Alzheimer's disease (AD, $n = 13$) were combined into AD/MCI due to the small number of participants in each group.

Abbreviations: CDR, Clinical Dementia Rating Scale; FMU, Fukushima Medical University; HA, healthy older adults; KPUM, Kyoto Prefectural University of Medicine; KU, Kyoto University; MMSE, Mini-Mental State Examination; NCNP, National Centre of Neurology and Psychiatry; PADNI, Parkinson's and Alzheimer's disease Dimensional Neuroimaging Initiative; PD, Parkinson's disease; TMMbMRI, Tohoku Medical Megabank Brain Magnetic Resonance Imaging study; mean ± standard deviation.

TMMbMRI dataset, the weighted sum of the PLS components chosen by the BAE model was back-projected onto each brain region for visualization (i.e., the BAE source map).

To test the generalizability of the TMMbMRI BAE model, we applied the model to predict brain ages of the PADNI HA group using a 10-fold CV (Figure 1). The number of components and weights of the PLS model were retrained using the entire TMMbMRI dataset. We applied the same BAE model to the PADNI PD and PADNI AD/MCI groups and compared the BAG. The bias correction was applied to the PADNI BAE. Hereafter, we describe the bias-corrected BAG unless otherwise mentioned.

To assess the effect of gender on BAE, we applied the same procedure separately to men and women, but we did not find a difference in BAG between the two groups. We thus pooled the data from men and women in further analyses (Section 2 of Supporting Information and Table S3).

2.4 | Brain age gap source analysis and classification of disease labels

To assess the brain features that yielded the BAG, we extracted the PLS components from the MRI data of the PADNI cohort. We per-

formed a regression analysis of the PLS components with age, which yielded the residuals of the PLS components that produced the BAG. The residuals were then back-projected onto the brain regions, which resulted in BAG source vectors that corresponded to the 167 features. The BAG source vectors in each brain region were standardized as z-scores using the mean and variance computed from the TMMbMRI data. These vectors are hereafter referred to as the BAG source.

We built classifiers to determine the group label of each PADNI participant using the BAG source as the feature. The classifiers were trained to discriminate between the following pair of group labels: AD/MCI versus HA, and AD/MCI versus PD. We randomly selected data from the pool of HA or PD datasets iteratively 100 times, so that the dataset size of the HA or PD subsamples matched the dataset size of the AD/MCI subsample. This avoided classification bias due to unmatched sample sizes. A stratified 10-fold CV was performed for validation. After the feature selection with the random forest classification, a linear support vector machine (SVM) was used to classify these disease labels. We calculated the performance measures in each iteration. The details of this content are provided in Section 3 of Supporting Information.

To gain insight into the classification results using the BAG source, we visualized the data structures of the BAG source. We reduced the dimension of the BAG source using t-distributed stochastic
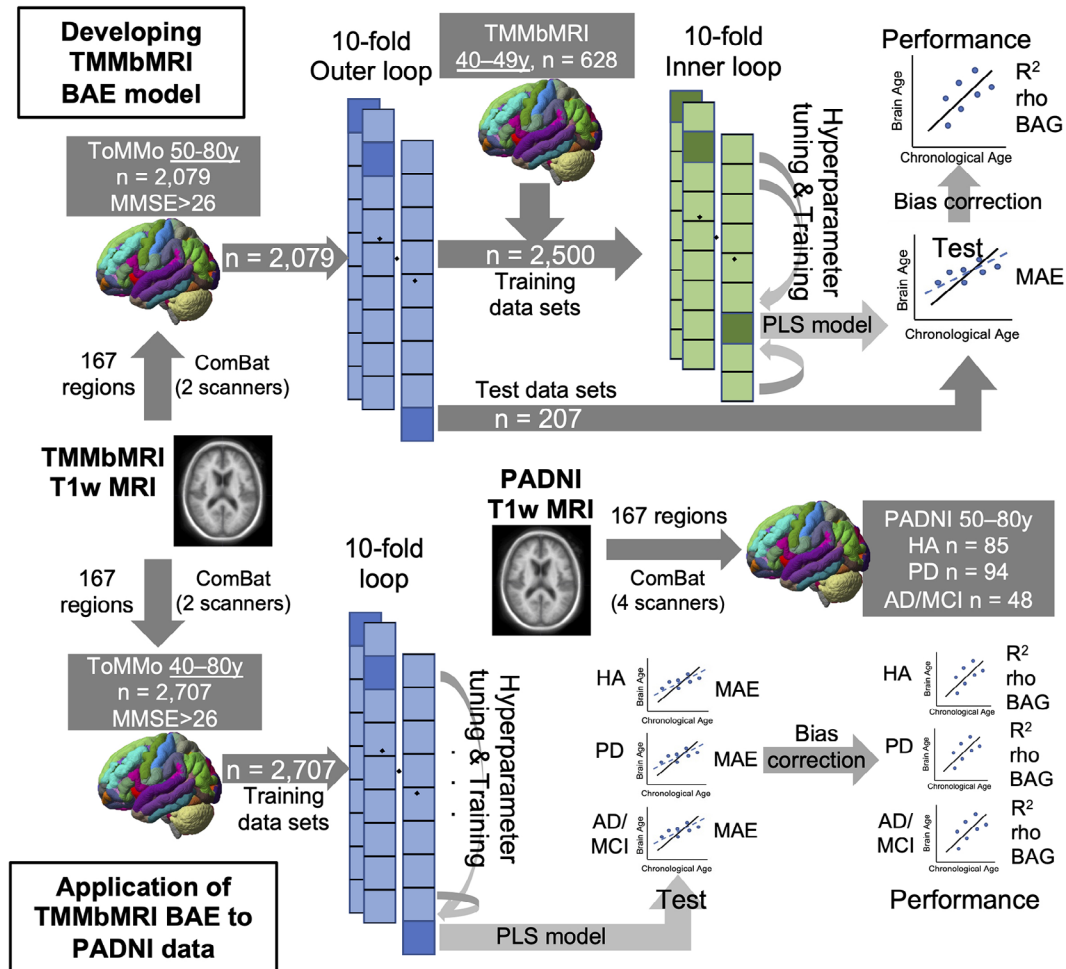
FIGURE 1 Analysis pipelines and validation schemes of brain age estimation (BAE) (upper panels). The brain age estimation (BAE) model was constructed using a partial least square regression (PLS) with a nested 10-fold cross-validation (CV). We used 167 features (cortical thickness and subcortical volumes) extracted from T1-weighted (T1w) magnetic resonance imaging scans (MRIs) of cognitively unimpaired (Mini-Mental State Examination [MMSE] score > 26), community-dwelling individuals in the Tohoku Medical Megabank Brain MRI (TMMbMRI) study. We used MRIs from individuals older than 40 years for hyperparameter tuning and training and applied the trained BAE to people aged ≥50 years for performance testing with mean absolute error (MAE) and R^2, rho, and brain age gap (BAG) (lower panels). The TMMbMRI BAE was applied to the Parkinson's and Alzheimer's disease Dimensional Neuroimaging Initiative (PADNI) individuals (aged ≥ 50 years), including healthy older adults (HA), Alzheimer's disease (AD), mild cognitive impairment (MCI), and Parkinson's disease (PD), collected from four sites after ComBat harmonization. Note that MCI and AD were combined and treated as a single group (AD/MCI) due to the small number of participants

neighbor embedding (t-SNE) with a perplexity value of 10 (Matlab R2020a, Mathworks, USA) and subsequently compared the t-SNE plots across the groups. For the reason stated later (Section 3.4), in the t-SNE space, we constructed a linear SVM classifier to differentiate between AD/MCI and HA groups, subsequently applying this classifier to the PD group.

We projected the BAG source back onto the original brain regions (i.e., the BAG attribution map) and compared the BAG attribution maps among the groups. We first averaged the z-scores of the BAG source across all the participants in each group. The averaged z-scores were then converted into ascending rank order within each group to generate the BAG attribution maps. This method was used to compare ranks between group pairs, which allowed us to compare BAG attribution maps between the groups.

2.5 | Statistical analyses

A chi-squared test was used to compare the distribution of categories, such as sex, among groups. A one-way analysis of variance (ANOVA) was used to compare the BAG among the PADNI groups, followed by post hoc tests between groups using Holm's adjustment[30] for multiple comparisons. We used Spearman's correlation (rho) between the BAG and clinical and cognitive test scores of the PADNI cohort. Classification performance was assessed by averaging the performance metrics, including accuracy, recall, precision, F1 score, and the area under the receiver operating characteristic curve (AUC). We computed partial eta, Cohen's d, and rho as a measure of the effect size when applicable. We used Python version 3.8.2 for these analyses.
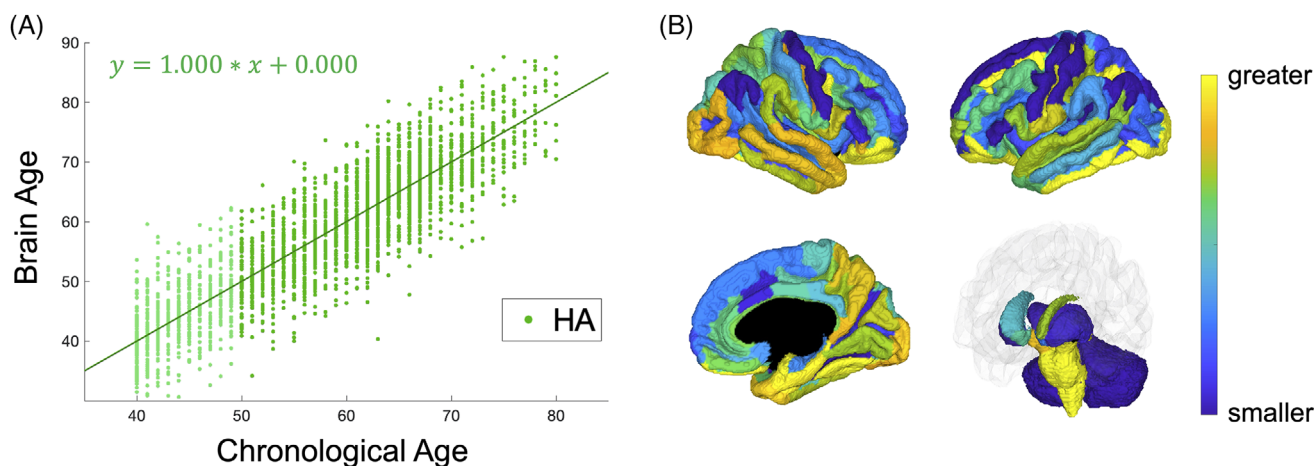
(A)

$y = 1.000 * x + 0.000$

(B)

FIGURE 2 Brain age estimation (BAE) based on 2707 community-dwelling people in the Tohoku Medical Megabank Brain MRI (TMMbMRI) study. (A) A plot of the brain age against the chronological age. Each dot represents an individual. The green line represents a regression line. The participants aged 40–50 years are represented in light green. (B) Weighted sum of the partial least squares regression components of our BAE model, back-projected onto brain regions (BAE source map). Yellow- and blue-colored regions have a higher and lower contribution to BAE, respectively

3 | RESULTS

3.1 | Brain age estimation in community-dwelling people in the TMMbMRI

The optimal number of components was eight. The TMMbMRI BAE model yielded an MAE of 4.95. R^2 and the BAGs were 0.41 and 0.00 ± 5.26 after bias correction (Figure 2A). The BAE source map (Figure 2B) indicated that the fronto-temporo-parietal association cortices, especially the posterior cingulate cortex/precuneus, ventral prefrontal cortex, and the lateral and medial temporal lobe (LTL/MTL) were the major contributors to our BAE model, while the contribution of the precentral and postcentral gyri, putamen, and cerebellum was relatively small.

3.2 | Generalization of the BAE model to the PADNI cohort

The TMMbMRI-based BAE model yielded an MAE of 5.01 in the PADNI HA. The BAG did not differ between the PADNI HA and the TMMbMRI (Cohen's $d = 0.05$, $t = -0.42$, $P = 0.67$). Other measures following bias correction showed that the TMMbMRI BAE model could be generalized to the PADNI HA group reasonably well (Table 2 and Figure 3).

3.3 | Brain age gap in PADNI cohort individuals with neurodegenerative disorders

We applied the BAE model to the PADNI PD and AD/MCI groups (Table 2 and Figure 3). One-way ANOVA revealed differences in the BAG among the PADNI HA, PD, and AD/MCI groups (partial eta = 0.053, $F(2, 224) = 6.212$, $P = 0.002$). The AD/MCI group showed

TABLE 2 Results from the application of the TMMbMRI brain age estimation model to the PADNI data

Parameter	R^2	Rho	BAG
PADNI HA	0.60	0.84	0.24 ± 5.13
PADNI PD	0.56	0.85	1.47 ± 4.51
PADNI AD/MCI	0.13	0.72	3.32 ± 4.79

Note: Results of correlation analysis between chronological ages and estimated brain ages.
Abbreviations: AD/MCI, Alzheimer's disease/mild cognitive impairment; BAG, brain age gap, mean ± standard deviation; HA, healthy older adults; PADNI, Parkinson's and Alzheimer's disease Dimensional Neuroimaging Initiative; PD, Parkinson's disease; R^2, coefficient of determination; *rho*, correlation coefficient; TMMbMRI, Tohoku Medical Megabank Brain MRI.

a larger BAG than the HA group (Cohen's $d = 0.61$, $t = 3.376$, $P = 0.003$, significant after Holm's adjustment). The AD/MCI group showed a lower R^2 compared to the other groups. The difference in BAG was also significant between the PD and AD/MCI group (Cohen's $d = 0.40$, $t = 2.253$, $P = 0.05$), but not between the PD and HA group (Cohen's $d = 0.25$, $t = 1.689$, $P = 0.09$).

In the PADNI cohort, we found a correlation between the BAG and all cognitive scores: MoCA ($rho = -0.225$, $P = 0.001$), WMS-R LM-IR ($rho = -0.277$, $P < 0.001$), WMS-R LM-DR ($rho = -0.262$, $P < 0.001$), WMS-R VR-IR ($rho = -0.154$, $P = 0.021$), and WMS-R VR-DR ($rho = -0.206$, $P = 0.002$; Figure S2). However, we did not find a significant correlation between the BAG and the MDS-UPDRS Part III score ($rho = 0.097$, $P = 0.153$).

3.4 | Disease classification using multivariate brain age gap source features

The SVM classifier, based on multivariate BAG source features, achieved a fair performance of 75%–80% for discriminating between
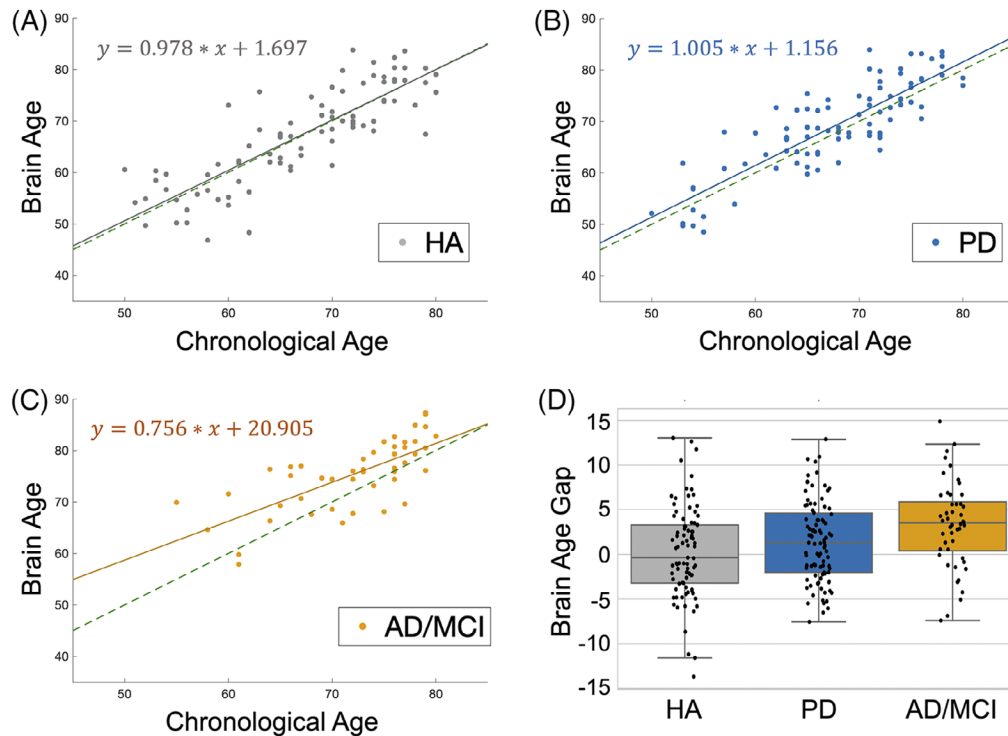
FIGURE 3 Application of the brain age estimation (BAE) model of the Tohoku Medical Megabank Brain MRI (TMMbMRI) data to the dataset of the Parkinson's and Alzheimer's disease Dimensional Neuroimaging Initiative (PADNI) cohort. Plots of the brain age against the chronological age in (A) healthy older adults (HA), (B) Parkinson's disease (PD), and (C) Alzheimer's disease/mild cognitive impairment (AD/MCI). The green dotted lines are the regression lines estimated by the TMMbMRI BAE. Solid lines are regression lines estimated by each group's data. (D) Boxplots of the brain age gaps were computed from each group's data. Boxes represent the interquartile range of the 25th and 75th percentile. Whiskers represent 1.5 times of the interquartile range. Each dot represents each person (A–D).

AD/MCI patients and HAs (accuracy = 0.756 ± 0.004, precision = 0.804 ± 0.005, recall = 0.704 ± 0.006, f1 = 0.735 ± 0.005, and AUC = 0.810 ± 0.005). However, the SVM classifier showed a modest performance of approximately 60% accuracy for differentiating between AD/MCI and PD patients (accuracy = 0.591 ± 0.004, precision = 0.594 ± 0.005, recall = 0.662 ± 0.006, f1 = 0.610 ± 0.005, and AUC = 0.601 ± 0.006).

We conducted the t-SNE analysis to determine the data structure of the BAG source. In the 2D t-SNE space (Figure 4A), although the AD/MCI and HA data formed segregated clusters, the distribution of the PD data was widespread, overlapping the AD/MCI and HA clusters (Figure 4B). Thus, we subdivided the PD group using the SVM classifier built for classifying AD/MCI and HA individuals in the t-SNE space. This AD/MCI-HA classifier divided the PD patients into two subgroups: PD classified as AD/MCI (PD_{AD}, $n = 46$) and PD classified as HA (PD_{HA}, $n = 48$). The difference in BAG was significant between the PD_{AD} and HA group ($P = 0.010$), and between the PD_{AD} and PD_{HA} ($P = 0.010$), but not between the PD_{HA} and HA group ($P = 0.906$). When we compared the cognitive and clinical scores between the PD subgroups (Figure 4C and Table S4), the PD_{AD} group showed poorer cognitive performance than the PD_{HA} group ($P = 0.036$ for the MoCA; $P < 0.001$ for the WMS-R LM-IR; $P = 0.0017$ for the WMS-R LM-DR; $P = 0.117$ for the WMS-R VR-IR; $P = 0.012$ for the WMS-R VR-DR, significant except for the VR-IR score). However, there was no significant difference in the CDR

($P = 0.926$), Hoehn and Yahr Scale ($P = 0.853$), and MDS-UPDRS Part III score ($P = 0.926$) between the PD_{AD} and PD_{HA} groups (after the Holm's adjustment). All effect sizes are presented in Table S4.

3.5 | Brain regions contributing to the difference in brain age gap

The rank-ordered BAG attribution map characterized the spatial distribution of brain regions affected by AD/MCI, PD, or both, beyond normative aging (Figure 4D–F and Table S5). For the AD/MCI group, excess cortical thinning beyond that observed in normative aging was prominent in the LTL/MTL, followed by the frontal and parietal association cortices and limbic regions. In the PD_{HA} group, the involvement of the subcortical, orbitofrontal, and ventral visual areas was evident, while the similar age-disproportionate thinning (e.g., LTL/MTL) to the AD/MCI group was also observed. In the PD_{AD} patients, the pattern of cortical thinning resembled that in the AD/MCI patients (Table S5). However, in the direct comparison between the AD/MCI and PD_{AD} groups, the AD/MCI was characterized by the involvement of the orbitofrontal, medial frontal, cingulate and middle/inferior temporal regions, whereas the PD_{AD} was characterized by the involvement of the primary sensorimotor and visual cortices (Figure 4D).
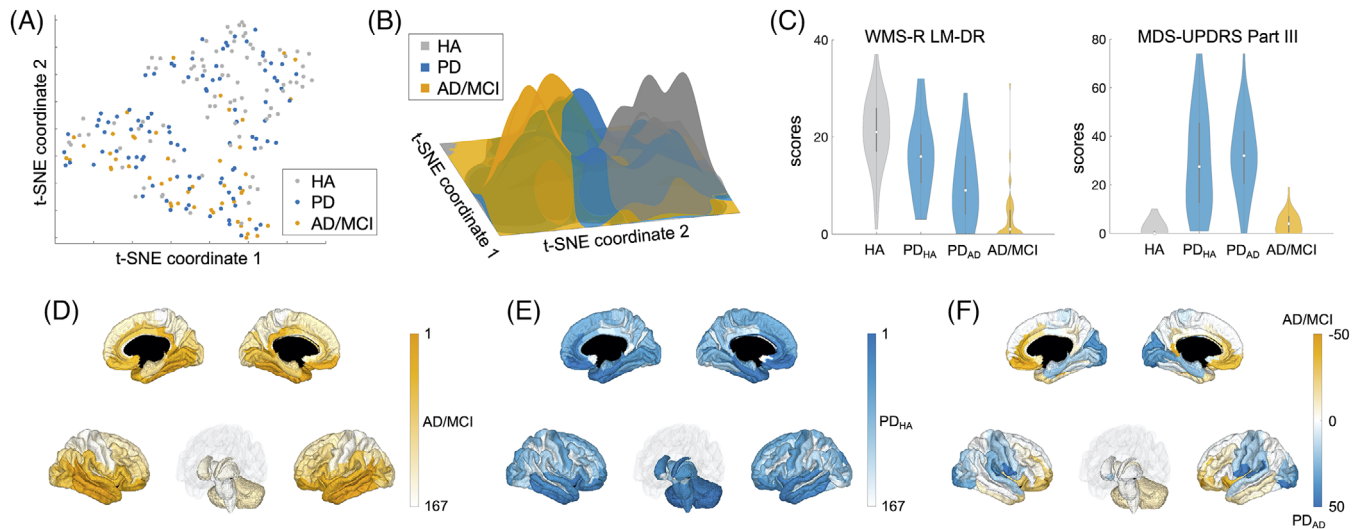
FIGURE 4 The t-distributed stochastic neighbor embedding (t-SNE) analysis and difference of contribution of the cortical thickness and subcortical volume. (A) 2D t-SNE plot of the brain age gap (BAG) source data in the Parkinson's and Alzheimer's disease Dimensional Neuroimaging Initiative (PADNI) healthy older adults (HA), Parkinson's disease (PD), and Alzheimer's disease/mild cognitive impairment (AD/MCI). (B) Probability density distribution of the AD/MCI, PD, and HA data. The probability density distribution was estimated from the 2D t-SNE plot in (A) using the kernel density estimation method. (C) Violin plots of scores of the delayed recall of logical memory in Wechsler Memory Scale-Revised (WMS-R LM-DR) and International Parkinson and Movement Disorder Society (MDS) -sponsored revision of Unified Parkinson's Disease Rating Scale, Part III (MDS-UPDRS Part III) in HA, PD classified as HA (PD_{HA}), PD classified as AD/MCI (PD_{HA}), and AD/MCI. (D) Ranks of BAG sources of the AD/MCI projected back onto each brain region (BAG attribution map). Small numbers represent more severe involvement. (E) BAG attribution map of PD_{HA}. (F) Across-group BAG attribution map for AD/MCI and PD_{AD} (AD—PD_{AD}). Orange color represents more severe involvement in AD/MCI while blue color in PD_{AD}.

4 | DISCUSSION

We developed an interpretable PLS-based BAE technology to assess normative senescence-related brain atrophy. We found significantly higher BAGs in the AD/MCI patients. BAGs were not significantly higher in the PD patients than in the HAs. However, based on BAG sources, PD patients were sub-grouped into two cognitively distinct groups (i.e., PD_{AD} and PD_{HA}), and BAGs were significantly higher in the PD_{AD} than the HAs.

4.1 | Toward interpretable brain age estimation

Despite advances in BAE technology,[4,5] previous studies have seldom offered interpretable information about the specific brain regions that contribute to BAE. Recently, studies on deep learning-based BAE have used saliency maps[31–33] (generated using all MRI information, including non-parenchymal structures) that are not directly linked to neurobiological interpretations. Therefore, one of our primary aims was to visualize regional information on cortical thickness and ScV, which have been reported to best characterize the effects of aging.[34] The BAE source map revealed thinning of the fronto-temporo-inferior parietal association cortices, whereas the cortical thickness of the primary motor and sensory cortices and the ScV of the basal ganglia and cerebellum were relatively preserved. Previous histological examinations have demonstrated this contrast between age-related changes in

association cortices and primary cortices,[35] supporting the plausibility of our BAE source map.

4.2 | Utility of the brain age gap for neurodegenerative disorders

Aging is the top risk factor for most neurodegenerative disorders Thus, capturing the disease effects cannot be achieved without considering the neurobiology of aging. Typically, age effects are removed using statistical models. However, this process not only removes age effects but also disease effects, at least partially. In contrast, the BAE approach removes only the effects of normative aging, while retaining the effects of disease as BAG-related components. Therefore, this BAE approach is considered effective for isolating the effects of neurodegenerative disease from the effects of aging.

While the BAG was significantly higher in the AD/MCI group than in the HA group, the BAG of the PADNI AD/MCI was mildly smaller than that of AD/MCI patients reported in the literature.[7–12,16,31,33,36] This may be because our AD/MCI group probably included a continuum from mild MCI to AD. Supporting this, the BAGs were more variable in the AD/MCI group than in the other groups (Figure 3). Because the BAG was closely associated with cognitive impairment in our results, it is likely that the variance in cognitive impairment accounts for this large variance of the BAGs in the AD/MCI group.

The BAG was not significantly higher in the PD group than in the HA group, while the BAG in the PD group was consistent with findings reported in recent studies on PD.[11,13,14] However, PD patients classified as AD/MCI in the t-SNE space (PD$_{AD}$) exhibited significantly higher BAGs than both the HA and PD patients classified as HA (PD$_{HA}$). Additionally, the PD$_{AD}$ demonstrated greater cognitive impairment compared to the PD$_{HA}$. Interestingly, there was no significant difference in the CDR between these groups. Therefore, the BAG may serve as a cognitive marker in the diagnosis of PD subtypes.

The BAG was correlated with many cognitive scores but not with the MDS-UPDRS score. An explanation is that cognitive decline was predominantly influenced by neuromorphological changes modeled by BAE that were continuous to the changes underlying AD/MCI. In contrast, motor impairment is mainly affected by functional alterations, including dopamine deficiency in normal aging[37] and PD. From another perspective, the BAG might be less sensitive to the neuromorphological changes of PD because the BAE model weighted less on the motor-related areas than the cognitive-related areas, as seen in the BAG source map. Accordingly, structural alterations related to motor symptoms in PD could be less reflected in the BAG. The BAG may primarily serve as a metric for assessing systems involved more in cognitive functions than motor impairments; however, we emphasize that, if we analyzed the source of BAG, the BAE is useful also in detecting parkinsonism and cognitive disturbance embedded in the PD spectrum.

4.3 | Disease classification with BAG-related information and attribution maps

We demonstrated that visualizing the data structure of the BAG source would enhance our understanding of the mechanisms underlying the overlap and segregation of AD and PD pathophysiology. Specifically, by applying t-SNE to visualize the BAG sources, we found that PD patients were subclassified into two groups: one overlapping with AD/MCI (PD$_{AD}$) and the other overlapping with healthy aging (PD$_{HA}$). The PD$_{AD}$ showed greater cognitive decline than PD$_{HA}$, while no significant difference in the Hoehn and Yahr Scale and MDS-UPDRS Part III score. These results suggest that the BAG analysis can classify PD patients into these clinically distinct subtypes that cannot be explained by differences in disease progression: one subtype may represent PD without cognitive impairment, while the other may represent PD with cognitive impairment.[38] Interestingly, the PD group exhibited more consistent BAGs, while the distinct two clusters emerged based on the BAG source, suggesting that different cortical thinning patterns can exist within similar BAGs in PD. On the other hand, the AD/MCI group is widely distributed within a single cluster in the t-SNE space. This finding supports the notion that, in contrast to PD, both AD and MCI are disorders that exist along a continuous spectrum[39] with respect to neuromorphological features.

We found a differential BAG source pattern between the AD/MCI and PD$_{AD}$ groups. The BAG attribution map revealed greater thinning of the primary sensorimotor area and visual cortices in the PD$_{AD}$ compared to the AD/MCI. This finding is plausible given the motor

and visual symptoms in PD, and is consistent with previous studies on PD and DLB.[40-43] On the other hand, the AD/MCI exhibited greater thinning of the medial frontal, cingulate, and middle/inferior temporal regions, which are closely associated with the default mode network, a critical network in the pathophysiology of AD.[44] These findings suggest that the BAG source analysis has the potential to extract neuromorphological changes specific to neurodegenerative disorders.

4.4 | Study limitations and future perspectives

We admit certain limitations in the definition of cohort participants, particularly with respect to the criteria for healthy participants and the subclassification of MCI.[45] We also emphasize the need for methodological refinements in our BAE model, including improvements to the algorithms and consideration of additional potential factors. The details are provided in Supporting Information.

5 | CONCLUSIONS

The BAG is a useful summary indicator of brain states underlying cognitive/behavioral decline in dementia syndrome and other neuropsychiatric disorders. Furthermore, the BAG source analysis can provide us with enriched spatial information with disease specificity. We believe that the proposed approach could pave the way toward applying large-scale data to the screening or diagnostic support of neurodegenerative disorders.

CONFLICT OF INTEREST STATEMENT

The authors declare no conflicts of interest. Author disclosures are available in the Supporting Information.

DATA AVAILABILITY STATEMENT

The data that support the findings of this study are available from the corresponding author upon a reasonable request.

CONSENT STATEMENT

Approval was obtained from each ethics committee. The procedures used in this study adhere to the tenets of the Declaration of Helsinki. All participants provided written informed consent according to the

protocol approved by each institute (NCNP A2018-089, KU C1435, KPUM 111x, and FMU 222x).

ORCID

Takashi Hanakawa https://orcid.org/0000-0003-3267-8214

REFERENCES

1. Bethlehem RaI, Seidlitz J, White SR, et al. Brain charts for the human lifespan. *Nature*. 2022;604(7906):525-533. doi:10.1038/s41586-022-04554-y
2. Sudlow C, Gallacher J, Allen N, et al. UK Biobank: an open access resource for identifying the causes of a wide range of complex diseases of middle and old age. *PLoS Med*. 2015;12(3):e1001779. doi:10.1371/journal.pmed.1001779
3. Caspers S, Moebus S, Lux S, et al. Studying variability in human brain aging in a population-based German cohort – rationale and design of 1000BRAINS. *Front Aging Neurosci*. 2014;6:149. doi:10.3389/fnagi.2014.00149
4. Cole JH, Franke K. Predicting age using neuroimaging: innovative brain ageing biomarkers. *Trends Neurosci*. 2017;40(12):681-690. doi:10.1016/j.tins.2017.10.001
5. Franke K, Gaser C. Ten years of BrainAGE as a neuroimaging biomarker of brain aging: what insights have we gained? *Front Neurol*. 2019;10:789. doi:10.3389/fneur.2019.00789
6. Boyle R, Jollans L, Rueda-Delgado LM, et al. Brain-predicted age difference score is related to specific cognitive functions: a multi-site replication analysis. *Brain Imaging Behav*. 2021;15(1):327-345. doi:10.1007/s11682-020-00260-3
7. Bashyam VM, Erus G, Doshi J, et al. MRI signatures of brain age and disease over the lifespan based on a deep brain network and 14 468 individuals worldwide. *Brain*. 2020;143(7):2312-2324. doi:10.1093/brain/awaa160
8. Li Y, Liu Y, Wang P, et al. Dependency criterion based brain pathological age estimation of Alzheimer's disease patients with MR scans. *BioMedical Engineering OnLine*. 2017;16(1):50. doi:10.1186/s12938-017-0342-y
9. Löwe LC, Gaser C, Franke K. Initiative for the ADN. The effect of the APOE genotype on individual BrainAGE in normal aging, mild cognitive impairment, and Alzheimer's disease. *PLoS One*. 2016;11(7):e0157514. doi:10.1371/journal.pone.0157514
10. Millar PR, Gordon BA, Luckett PH, et al. Multimodal brain age estimates relate to Alzheimer disease biomarkers and cognition in early stages: a cross-sectional observational study. In: Miller KL, Chin J, Cole J, Vidal-Pineiro D, eds *Elife*. 2023;12:e81869. doi:10.7554/eLife.81869
11. Beheshti I, Mishra S, Sone D, Khanna P, Matsuda H. T1-weighted MRI-driven brain age estimation in Alzheimer's disease and Parkinson's disease. *Aging Dis*. 2019;11(3):618-628. doi:10.14336/AD.2019.0617
12. Choi US, Park JY, Lee JJ, Choi KY, Won S, Lee KH. Predicting mild cognitive impairments from cognitively normal brains using a novel brain age estimation model based on structural magnetic resonance imaging. *Cereb Cortex*. 2023;33(21):10858-10866. doi:10.1093/cercor/bhad331
13. Charissé D, Erus G, Pomponio R, et al. Brain age and Alzheimer's-like atrophy are domain-specific predictors of cognitive impairment in Parkinson's disease. *Neurobiol Aging*. 2022;109:31-42. doi:10.1016/j.neurobiolaging.2021.08.020
14. Eickhoff CR, Hoffstaedter F, Caspers J, et al. Advanced brain ageing in Parkinson's disease is related to disease duration and individual impairment. *Brain Commun*. 2021;3(3):fcab191. doi:10.1093/braincomms/fcab191

15. Nenadić I, Dietzek M, Langbein K, Sauer H, Gaser C. BrainAGE score indicates accelerated brain aging in schizophrenia, but not bipolar disorder. *Psychiatry Res Neuroimaging*. 2017;266:86-89. doi:10.1016/j.pscychresns.2017.05.006
16. Cole JH, Marioni RE, Harris SE, Deary IJ. Brain age and other bodily 'ages': implications for neuropsychiatry. *Mol Psychiatry*. 2019;24(2):266-281. doi:10.1038/s41380-018-0098-1
17. Taira M, Mugikura S, Mori N, et al. Tohoku medical megabank brain magnetic resonance imaging study: rationale, design, and background. *JMA J*. 2023;6(3):246-264. doi:10.31662/jmaj.2022-0220
18. Matsuoka T, Narumoto J, Morii-Kitani F, et al. Contribution of amyloid and putative Lewy body pathologies in neuropsychiatric symptoms. *Int J Geriatr Psychiatry*. 2023;38(9):e5993. doi:10.1002/gps.5993
19. Matsuoka T, Oya N, Narumoto J, et al. Reduced pineal volume may be associated with amyloid pathology and not with putative Lewy body pathology. *J Neurol Neurosurg Psychiatry*. 2024;95(8):791-792. doi:10.1136/jnnp-2023-332252
20. Wakasugi N, Hanakawa T. It is time to study overlapping molecular and circuit pathophysiologies in Alzheimer's and lewy body disease spectra. *Front Syst Neurosci*. 2021;15:777706. doi:10.3389/fnsys.2021.777706
21. Kuriyama S, Yaegashi N, Nagami F, et al. The Tohoku Medical Megabank Project: design and mission. *J Epidemiol*. 2016;26(9):493-511. doi:10.2188/jea.JE20150268
22. McKhann GM, Knopman DS, Chertkow H, et al. The diagnosis of dementia due to Alzheimer's disease: recommendations from the National Institute on Aging-Alzheimer's Association workgroups on diagnostic guidelines for Alzheimer's disease. *Alzheimers Dement*. 2011;7(3):263-269. doi:10.1016/j.jalz.2011.03.005
23. Postuma RB, Berg D, Stern M, et al. MDS clinical diagnostic criteria for Parkinson's disease: MDS-PD Clinical Diagnostic Criteria. *Mov Disord*. 2015;30(12):1591-1601. doi:10.1002/mds.26424
24. Koike S, Tanaka SC, Okada T, et al. Brain/MINDS beyond human brain MRI project: a protocol for multi-level harmonization across brain disorders throughout the lifespan. *NeuroImage: Clinical*. 2021;30:102600. doi:10.1016/j.nicl.2021.102600
25. Destrieux C, Fischl B, Dale A, Halgren E. Automatic parcellation of human cortical gyri and sulci using standard anatomical nomenclature. *Neuroimage*. 2010;53(1):1-15. doi:10.1016/j.neuroimage.2010.06.010
26. Fischl B, Salat DH, Busa E, et al. Whole brain segmentation: automated labeling of neuroanatomical structures in the human brain. *Neuron*. 2002;33(3):341-355. doi:10.1016/S0896-6273(02)00569-X
27. Fortin JP, Cullen N, Sheline YI, et al. Harmonization of cortical thickness measurements across scanners and sites. *Neuroimage*. 2018;167:104-120. doi:10.1016/j.neuroimage.2017.11.024
28. Smith SM, Vidaurre D, Alfaro-Almagro F, Nichols TE, Miller KL. Estimation of brain age delta from brain imaging. *Neuroimage*. 2019;200:528-539. doi:10.1016/j.neuroimage.2019.06.017
29. Le TT, Kuplicki RT, McKinney BA, et al. A nonlinear simulation framework supports adjusting for age when analyzing BrainAGE. *Front Aging Neurosci*. 2018;10:317. doi:10.3389/fnagi.2018.00317
30. Aickin M, Gensler H. Adjusting for multiple testing when reporting research results: the Bonferroni vs Holm methods. *Am J Public Health*. 1996;86(5):726-728. doi:10.2105/AJPH.86.5.726
31. Yin C, Imms P, Cheng M, et al. Anatomically interpretable deep learning of brain age captures domain-specific cognitive impairment. *Proc Natl Acad Sci*. 2023;120(2):e2214634120. doi:10.1073/pnas.2214634120
32. Wood DA, Kafiabadi S, Busaidi AA, et al. Accurate brain-age models for routine clinical MRI examinations. *Neuroimage*. 2022;249:118871. doi:10.1016/j.neuroimage.2022.118871
33. Lee J, Burkett BJ, Min HK, et al. Deep learning-based brain age prediction in normal aging and dementia. *Nat Aging*. 2022;2(5):412-424. doi:10.1038/s43587-022-00219-7

34. Fjell AM, McEvoy L, Holland D, Dale AM, Walhovd KB. What is normal in normal aging? Effects of aging, amyloid and Alzheimer's disease on the cerebral cortex and the hippocampus. *Prog Neurobiol.* 2014;117:20-40. doi:10.1016/j.neurobio.2014.02.004

35. Chance SA, Casanova MF, Switala AE, Crow TJ, Esiri MM. Minicolumn thinning in temporal lobe association cortex but not primary auditory cortex in normal human ageing. *Acta Neuropathol.* 2006;111(5):459-464. doi:10.1007/s00401-005-0014-z

36. Gaser C, Franke K, Klöppel S, Koutsouleris N, Sauer H, Initiative ADN. BrainAGE in mild cognitive impaired patients: predicting the conversion to Alzheimer's disease. *PLOS ONE.* 2013;8(6):e67346. doi:10.1371/journal.pone.0067346

37. Seidler RD, Bernard JA, Burutolu TB, et al. Motor control and aging: links to age-related brain structural, functional, and biochemical effects. *Neurosci Biobehav Rev.* 2010;34(5):721-733. doi:10.1016/j.neubiorev.2009.10.005

38. Wen MC, Chan LL, Tan LCS, Tan EK. Mild cognitive impairment in Parkinson's disease: a distinct clinical entity? *Transl Neurodegener.* 2017;6(1):24. doi:10.1186/s40035-017-0094-4

39. Garcia Condado J, Cortes JM. NeuropsychBrainAge: a biomarker for conversion from mild cognitive impairment to Alzheimer's disease. *Alzheimers Dement.* 2023;15(4):e12493. doi:10.1002/dad2.12493

40. Lebedev AV, Westman E, Beyer MK, et al. Multivariate classification of patients with Alzheimer's and dementia with Lewy bodies using high-dimensional cortical thickness measurements: an MRI surface-based morphometric study. *J Neurol.* 2013;260(4):1104-1115. doi:10.1007/s00415-012-6768-z

41. Ye R, Touroutoglou A, Brickhouse M, et al. Topography of cortical thinning in the Lewy body diseases. *NeuroImage: Clinical.* 2020;26:102196. doi:10.1016/j.nicl.2020.102196

42. Blanc F, Colloby SJ, Philippi N, et al. Cortical thickness in dementia with Lewy bodies and Alzheimer's disease: a comparison of prodromal and dementia stages. *PLoS One.* 2015;10(6):e0127396. doi:10.1371/journal.pone.0127396

43. Galli A, Pilotto A, Chiarini B, et al. Occipital atrophy signature in prodromal Lewy bodies disease. *Alz & Dem Diag Ass & Dis Mo.* 2023;15(4):e12462. doi:10.1002/dad2.12462

44. Hojjati SH, Feiz F, Ozoria S, Razlighi QR. Alzheimer's disease neuroimaging initiative. topographical overlapping of the amyloid-β and tau pathologies in the default mode network predicts Alzheimer's disease with higher specificity. *J Alzheimers Dis.* 2021;83(1):407-421. doi:10.3233/JAD-210419

45. Garg N, Choudhry MS, Bodade RM. A review on Alzheimer's disease classification from normal controls and mild cognitive impairment using structural MR images. *J Neurosci Methods.* 2023;384:109745. doi:10.1016/j.jneumeth.2022.109745

SUPPORTING INFORMATION

Additional supporting information can be found online in the Supporting Information section at the end of this article.

APPENDIX A
LIST OF COLLABORATORS

Kyoto University Graduate School of Medicine

Atsushi Shima, Kiyoaki Takeda, Yuta Terada, Yusuke Sakato, Ikko Wada, Kenji Yoshimura, Akira Nishida, Haruhi Sakamaki-Tsukita, Koji Furukawa, Daisuke Kambe, Shiho Ubutaka, Masanori Sawamura, Etsuro Nakanishi, Hodaka Yamakado, Yasutaka Fushimi, Tomohisa Okada, Yuji Nakamoto, and Ryosuke Takahashi.

National Center of Neurology and Psychiatry

Yuji Takahashi, Harumasa Takano, Yohei Aoshima, Kazuaki Sajima, Kenji Hishikawa, Mayumi Inoue, Atsuko Inoue, Hiroko Fukuoka, Shinichiro Mogi, Kotaro Hattori, Kyoji Okita, Takashi Sakamoto, Tadashi Tsukamoto, Noriko Nishikawa, Yoshie Omachi, and Yohei Mukai.

Kyoto Prefectural University of Medicine

Fukiko Kitani-Morii, Fumitoshi Niwa, Masaki Kondo, Jin Narumoto, Kaeko Nakamura, Keisuke Shibata, Yukihide Nishimura, Ayu Imai, Nozomu Oya, Chikara Nakayama, Yuka Kato, Daisuke Ueno, Hiroyasu Ikeno, Jun Tazoe, Kentaro Akazawa, Kei Yamada, Nagara Tamaki, Tomoya Kotani, and Takeshi Nii.

Fukushima Medical University

Nozomu Matsuda, Toshiki Nakahara, Kasumi Hattori, Toshiki Nakahara, Hirooki Yabe, Naoto Kobayashi, Hiroshi Hoshino, Yuka Ueda, Yuya Hagane, Kazuko Kanno, Daisuke Goto, Wataru Toda, Yuhei Mori, Sinobu Kawakakatsu, Hiroshi Ito, Shiro Ishii, Ryo Yamakuni, Shinya Seino, Katuyuki Kikori, Hideaki Takasumi, Hironobu Ishikawa, Takashi Kanezawa, Emiya Koike, Yoshiki Endo, Anna Yamaki, Hiroshi Hayashi, Shigeyasu Sugawara, Naoyuki Ukon, Ayaka Nemoto, Minoru Oto, Yayoi Kurihara, and Yasuhiro Hashimoto.

Tohoku Medical Megabank Organization, Tohoku University

Masayuki Yamamoto, Kengo Kinoshita, Shinichi Kuriyama, Atsushi Hozawa, Naoko Mori, Makiko Taira, and Tomo Saito.